FLORE
Repository istituzionale dell'Università degli Studi di Firenze

Ionic liquids as diathermic fluids for solar trough collectors' technology: a corrosion study

(Article begins on next page)

04 May 2024

Ionic liquids as diathermic fluids for solar trough collectors' technology: A corrosion study

Ilaria Perissi[a,b,*], Ugo Bardi[a,b], Stefano Caporali[a,b], Alessio Fossati[a,b], Alessandro Lavacchi[a,b]

[a]*Dipartimento di Chimica, Università di Firenze, Via della Lastruccia 3, 50019 Sesto Fiorentino (FI), Italy*
[b]*Consorzio Interuniversitario Nazionale di Scienza e Tecnologia dei Materiali (INSTM), Unità di Ricerca di Firenze, 50147 Firenze, Italy*

Abstract

The AISI 304 and AISI 1018 steels (frequently used in solar collectors' plants) in contact with four different ionic liquids (ILs) suitable as diathermic fluids, were studied. Immersion tests were performed at $220\,^{\circ}C$ (the working temperature in such plants) for 10 days. The corrosion morphologies of the steels were investigated by scanning electron microscopy coupled with energy dispersive X-ray (EDX) microanalysis and the content of metals in the solution were detected via ICP-OES. The tests showed that the most performing IL is the ethyl-dimethyl-propyl-ammonium-bis(trifluoromethylsulphonyl)imide. The corrosion properties of the two alloys in contact with such IL were investigated by means of Tafel plots and resistance polarization at room temperature in open-to-air vessels.
© 2007 Elsevier B.V. All rights reserved.

Keywords: Solar collectors; Ionic liquids; Steels' corrosion; Tafel plots

1. Introduction

The depletion of fossil resources and the climate risks arising from their are serious concerns in the modern society. Finding a really durable, green and safe alternative to fossil fuel is one of the issues in which the scientific community is engaged. In the last few years, considerable progress has been made for solar power plants that use parabolic trough collectors' technology. The method is based on cylindrical parabolic mirrors that concentrate solar light onto a receiver pipe, running at the focus of the reflector. The collected heat is transferred to the heat exchangers by means of heat transfer fluids (HTF) that gather the heat due to irradiation and transfer it. The output of the plant may be electric power, but that is possible with good efficiency only for very large plants. For smaller and more effective applications, the heat can be used as a source of hot water or used in a "chiller" as

energy source for air conditioning for domestic or industrial applications. The scheme of a typical plant working on this principle is depicted in Fig. 1. The physical properties of such fluids play a fundamental role in the process yield. Actually, the HTF used in such plants are constituted by paraffinic or siliconic oils [1]. The fluids used as HTF had to satisfy a set of requirements such as: low vapour pressure, high thermal stability, 'green and safe properties' (biodegradability, no toxicity, no flammability), high thermal capacity and others. These requirements are very challenging and are not completely achieved by the products available in the market [2]. Ionic liquids (ILs) are a relatively new group of substances that match many of the thermophysical and chemical properties [3,4] required for efficient heat transfer and storage. However, for their use in solar thermal plants, an in depth knowledge of the corrosion properties in contact with the plant's material is mandatory. The purpose of the present work is to investigate the behaviour of some ILs, selected on the basis of their thermal and rheological properties, without and with contact with two different alloys (carbon steel and stainless steel) widely employed in thermal circuits (piping lines, heat exchangers, etc.).

*Corresponding author at: Dipartimento di Chimica, Università di Firenze, Via della Lastruccia 3, 50019 Sesto Fiorentino (FI), Italy. Tel.: +39554573119; fax: +39554573120.

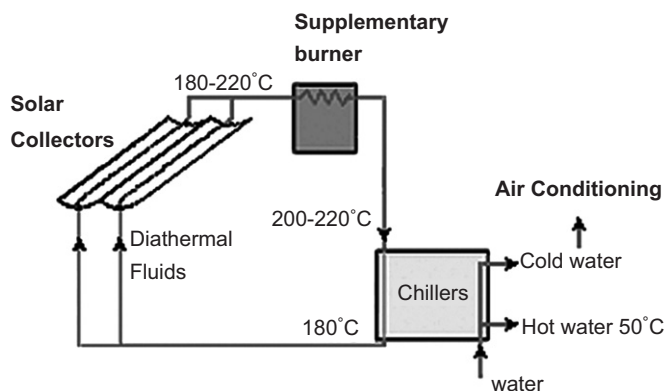*E-mail address:* ilaria.perissi@unifi.it (I. Perissi).

Fig. 1. Outline plan of a typical solar parabolic trough collectors field.

The investigation has been carried out by electrochemical, spectroscopic (ICP) and gravimetric techniques, while the morphological and chemical modifications of the alloys' surfaces after the interaction with the ILs, were monitored by scanning electron microscope (SEM) coupled with energy dispersive X-ray (EDX) microanalysis.

2. Experimental

2.1. Materials

Four ILs, specially designed for high-temperature applications, were supplied by Merck KGaA. They are: 1-hexyl-3-methylimidazolium tri(pentafluoroethyl)trifluorophosphate [HMImPF$_3$(C$_2$F$_5$)$_3$] (T_{dec} 300 °C, viscosity 74.30 mm^2 s^{-1} at 20 °C), 1-butyl-1-methylpyrrolidinium trifluoromethanesulfonate [BMPyF$_3$CSO$_3$] (T_{dec} 340 °C, viscosity 173.9 mm^2 s^{-1} at 20 °C), ethyl-dimethyl-propyl-ammonium bis(trifluoromethylsulphonyl)imide [EdMPNTf$_2$N] (T_{dec} 320 °C, viscosity 71.63 mm^2 s^{-1} at 20 °C), 1-butyl-1-methylpyrrolidinium bis(trifluoromethylsulphonyl)imide [BMPyTf$_2$N] (T_{dec} 310 °C, viscosity 71.50 mm^2 s^{-1} at 20 °C). As declared by the supplier, the maximum impurities present in these ILs are: chlorides (<1000 ppm) and water (<10,000 ppm). The molecular formulas of these ILs are depicted in Fig. 2. The ILs were tested alone and in contact with two different alloys: the AISI 1018 a carbon steel, 0.14–0.20 wt% C, 0.60–0.90 wt% Mn, 0.035 wt% P, 0.040 S, density 7.87 g cm^{-3} from McMaster-Carr, and the AISI 304 a stainless steel, Cr 17–20%, Mn <2%, Ni 8–11%, C <800%, density 7.93 g cm^{-3} from Goodfellow.

2.2. Gravimetric and ICP-OES analysis

Three samples of each alloy were prepared as thin disks (thickness <0.5 mm) and their faces grinded with SiC paper down to 1200 grit in order to achieve a reproducible surface finishing. The samples were weighed and then placed in 10 ml beakers, covered with the IL and placed in an oven at 220 °C for 48 h and for 10 days together with beakers containing 2 ml of the net ionic liquid. After the immersion tests, the alloys samples were washed with
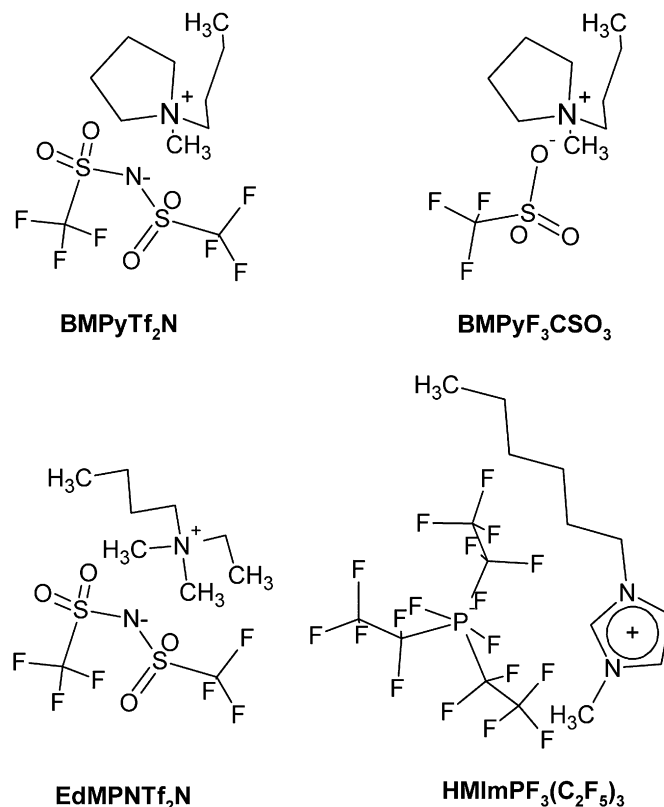

Fig. 2. Structures of the investigated ionic liquids.

acetone, dried under air and weighed again to calculate the weight loss, while the ILs were analysed via ICP-OES in order to determine the amount of dissolved metals. The matrix effect was corrected preparing "blank" solutions using the samples of ILs kept in the muffle without the contact with the metals. About 0.1 g of each ILs was added at 1 ml of 'aqua regia' and gently heated (80 °C) for few minutes in order to allow their complete dissolution. The solutions obtained were transferred in a "class A" volumetric flask (100 ml) and filled with distilled water. The measures were performed using a Dv OES Perkin-Elmer Optima 2000 with multielements method. Analytical conditions were as follows: RF power at 1350 W; Plasma flow at 20 l min^{-1}, Neb. flow at 0.80 l min^{-1}; Aux 0.5 l min^{-1}; view distance for axial view was set at 15 mm and sample flow rate at 15 l min^{-1}.

2.3. SEM and EDX analysis

After cleaning and weighing, the surface of the samples was examined by SEM–EDX using an ISI 100B microscope with an NSS300 microanalysis by Thermo Electron Corporation. The acceleration voltage was 25 kV, and the acquired peaks were fitted by Gaussian-type curves applying the Proza (Phi-Rho-Z) correction method. In order to determine the average surface composition the values were obtained by averaging the results of nine independent measures performed on three spots (50 × 50 μm^2) randomly chosen on every sample.

2.4. Electrochemical measurements

The electrochemical investigation was carried out using a Potentiostat/Galvanostat PARSTAT® 2273, Ametek Inc, employing a small-volume Teflon® cell (about 3 ml) built in our laboratory. The counter-electrodes (CE) and reference electrodes (RE) were constituted by platinum wires (99.9% Goodfellow), while the working electrodes (WE) were constituted by disks prepared as for the gravimetric experiments. The geometric area exposed was $50\,mm^2$ and the samples were placed as close as possible ($<1\,mm$) to the RE in order to minimize the ohmic drop.

3. Results

3.1. Immersion tests and EDX analysis

3.1.1. Forty-eight hours immersion tests at 220 °C

The tests performed in open vessels at 220 °C evidenced the formation of an adherent dark layer on the sample's surfaces just after 48 h of immersion for three of the four investigated ILs. The resulting layers not removable by sonication and acetone rinsing (see Fig. 3b). Moreover, the colours of the ILs, independent of the presence of metals, changed to dark brown. Apparently, such observation is in disagreement with the literature data, where much higher decomposition temperatures are reported. However, these values were obtained via DSC or TGA, heating the material for much shorter times as recently observed by Kroon et al. [5]. Furthermore, recent studies demonstrate that the decomposition of ILs can be also speeded up by the presence of metals in contact with [6,7].

The morphology of the interaction layers depends on the nature of the IL as well as the metal in contact as shown in Fig. 5, while their chemical composition, as determined by EDX, results constituted by C, N, O, S, P, F and the metals present in the alloys. A special attention was paid to sulphur, phosphorous and fluorine that are unambiguously derived from the ILs.

The EDX results are summarized in Fig. 6 where each bar of the histograms represents the F, S and P content (wt%), respectively, found on the surface of the AISI 304 and AISI 1018. The data are obtained excluding the highest and the lowest values and the data range is displayed by the thin line superimposed. Regarding $BMPyTf_2N$, the ratio between sulphur and fluorine does not respect the stoichiometry of the Tf_2N ion (1:3); but it is nearly 1:1, suggesting the breaking down of the molecule's structure. Only the samples immersed in $EdMPNTf_2N$ showed no evident contamination and the surface's morphology remains practically unchanged (Figs. 4b, 5c and d). In this case the fluorine and the sulphur contents on the surface layer are very low, approaching the detection limit for this technique. Therefore, these data did not constitute substantial proof of residual absorption of the IL (Fig. 6).

About the test in $BMPyF_3CSO_3$ the EDX analysis shows that the fluorine and the sulphur are about 1 and 5 wt%, respectively, and the interaction layer appears more fragile with respect to $BMPyTf_2N$ (Fig. 5e and f) for both the steels. Also the $HMImPF_3(C_2F_5)_3$ degraded, in accordance with the observation of Baranyai et al. [8], forming a dark, thin and adherent interaction layer (Fig. 5g and h). In such samples the fluorine content was ranging from 4 to 12 wt%, while the phosphorus was found ranging between 1 and 2 wt%.

This preliminary test allows us to assess the impossibility to use the $BMPyF_3CSO_3$, $BMPyTf_2N$ and $HMImPF_3(C_2F_5)_3$ as diathermic fluids for solar trough collectors in open-to-air condition, owing to the low stability showed at the typical working temperature (220 °C). Therefore, we decide to extend the immersion test, for 10 days, only on the $EdMPNTf_2N$ and $BMPyTf_2N$, which share the same anion, in order to compare the effect of the cation in the corrosion properties.
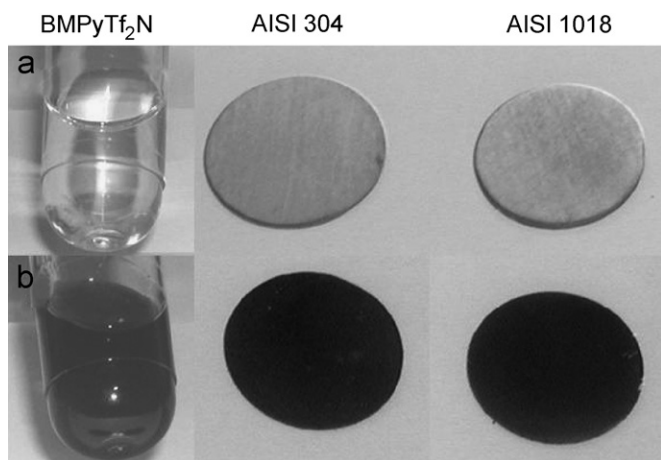

Fig. 3. Net $BMPyTf_2N$ (a) before and (b) after the 48 h tests at 220 °C (similar are the solutions stayed in contact with the alloys); also the two alloys samples are shown: (a) before the immersions and (b) after the immersions.

Fig. 4. Net $EdMPNTf_2N$ (a) before and (b) after the 48 h tests at 220 °C (similar are the solutions stayed in contact with the alloys); also the two alloys samples are shown: (a) before the immersions and (b) after the immersions.
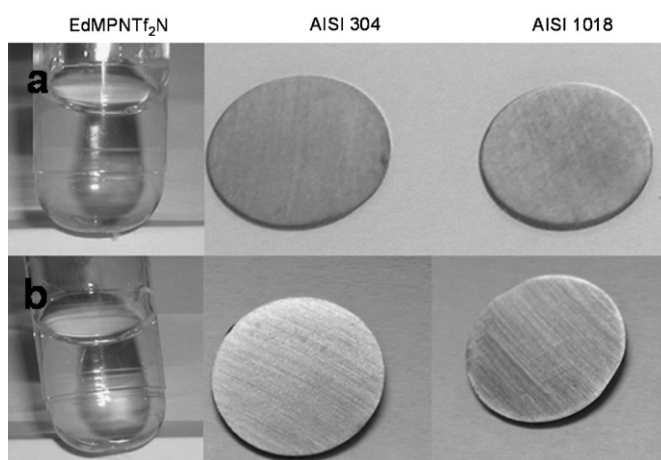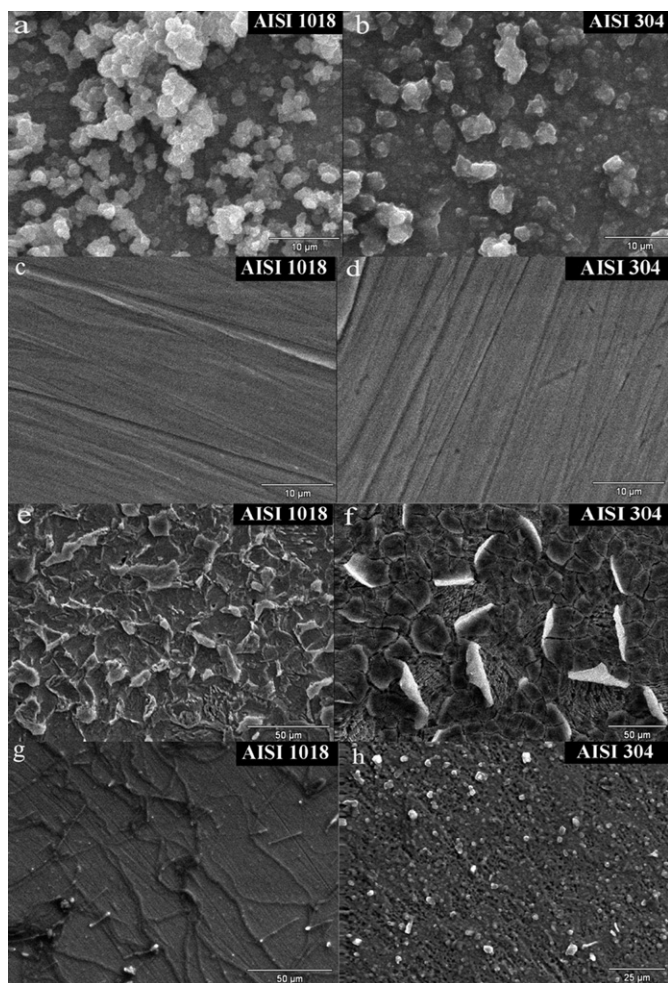
Fig. 5. SEM micrographs of the steels after 48 h immersion test at 220 °C in: (a, b) $BMPyTf_2N$; (c, d) $EdMPNTf_2N$; (e, f) $BMPyF_3CSO_3$; (g, h) $HMImPF_3(C_2F_5)_3$.

3.1.2. Ten days immersion tests at 220 °C

After 10 days at 220 °C the samples of both the steels immersed in the $BMPyTf_2N$ showed an increase of the dark layer's thickness. At the same time, these layers become rich in fluorine and sulphur, whose wt% were ranging from 10 to 25 wt% (Fig. 7), strengthening the hypothesis that the IL's decomposition proceeds together with the time of exposure. On the contrary, the samples immersed in $EdMPNTf_2N$ show an almost constant content of these elements even after such long time, suggesting a higher thermal stability of such IL in the investigated conditions with respect to the others. However, localized corrosion phenomena are now clearly detectable on the surface of both the alloys (Fig. 8).

In order to determine the corrosion rate, the amount of metals dissolved in the ILs, the solutions deriving from the 10-days immersion tests in $EdMPNTf_2N$ and $BMPyTf_2N$ were analysed by the ICP-OES (Table 1). The concentration of the metals found in $EdMPNTf_2N$ is low indeed, justifying the invariability in the weight-loss test. Nevertheless, these values are consistent with the observed localized corrosion phenomena occurring at the alloy surface. The estimated corrosion rates are around $1.23 \times 10^{-2}\,g\,cm^{-1}\,yr^{-1}$ for AISI 304 and $1.79 \times 10^{-2}\,g\,cm^{-1}\,yr^{-1}$ for AISI 1018. Surprisingly, the metals' content in $BMPyTf_2N$ was even lower, resulting under the detection level. We think that the interaction layer present on the samples is capable of shielding the surface from the solution, preventing the metals release. The formation of such layer is also the reason for the weight gain observed after the immersion test (about 3.5% after 10 days).

Looking at the market of HTF (glycol, aromatics, petroleum derivate oils), it is well known that oxidation usually occurs at temperature above 100 °C when the fluids come in contact with air [9]. Also more performing fluids, as siliconic oils derivates, gelatinized around 180–200 °C in
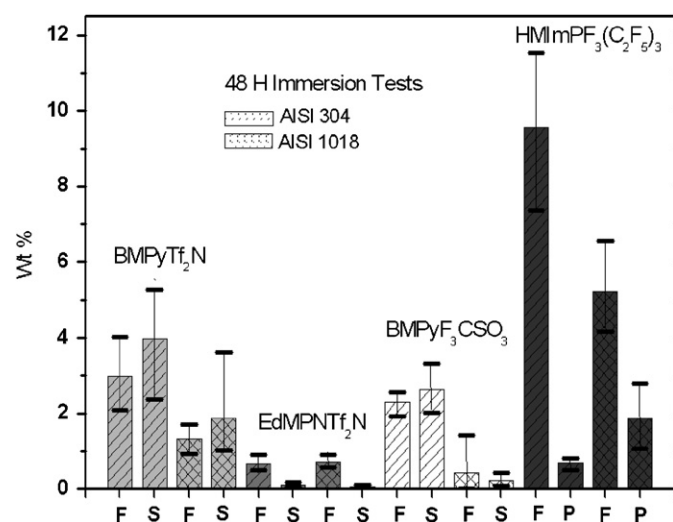

Fig. 6. F, S and P wt% on the AISI 1018 (grid lines filled histograms) and the AISI 304 (inclined lines filled histograms) surfaces after 48 h immersion tests at 220 °C in the investigated ILs.
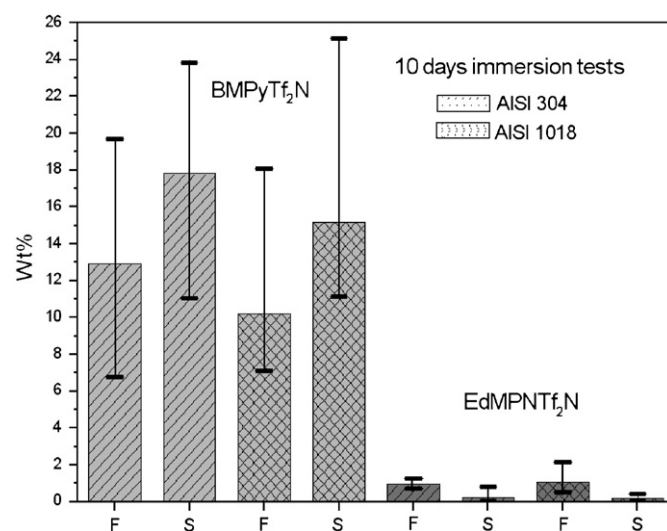

Fig. 7. F and S wt% on the AISI 1018 (grid lines filled histograms) and the AISI 304 (inclined lines filled histograms) surfaces after 10 days immersion tests at 220 °C in $BMPyTf_2N$ and $EdMPNTf_2N$.
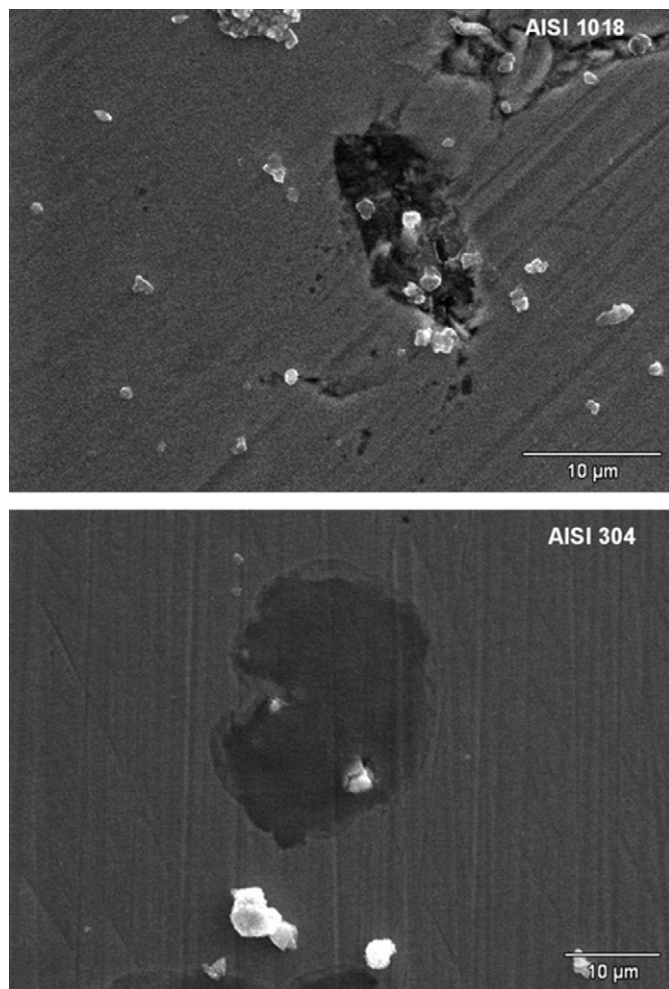
Fig. 8. Localized corrosion phenomena on the AISI 304 and the AISI 1018 specimens after 10 days immersion tests at 220 °C in EdMPNTf$_2$N.

Table 1
Metals' concentrations by ICP-OES analysis find in the ILs solutions deriving from the alloys' 10 days immersion tests

Alloy	Cr (mg kg$_{IL}^{-1}$)	Fe (mg kg$_{IL}^{-1}$)	Mn (mg kg$_{IL}^{-1}$)	Ni (mg kg$_{IL}^{-1}$)
EdMPNTf$_2$N				
AISI 304	54.7	181.7	–	30.1
AISI 1018	–	260.9	5.2	–
BMPyTf$_2$N				
AISI 304	Not detected	Not detected	–	Not detected
AISI 1018	–	Not detected	Not detected	–

open-to-air condition. Thus, compared with such commercial liquids, the EdMPNTf$_2$N presents better performance in terms of *sludge build up*.

3.2. Room temperature electrochemistry measurements

In order to shed some light on the corrosion mechanism and to evaluate the relevance of corrosion phenomena at room temperature, we performed an investigation via electrochemical techniques.

3.2.1. Stability of RE

In order to evaluate the stability of the Pt wire as quasi-RE we test its behaviour with respect to the Ferrocene/Ferrocenium redox couple (5 mM solution) in aerated EdMPNTf2N [10]. The CVs obtained on glassy carbon electrode ($\varnothing$ 3 mm) are comparable to the curves reported in the literature for similar ILs [11–13] characterized by an almost reversible one-electron oxidation process. The curves recorded immediately after the immersion of the electrodes after 9 and 22 h are shown in Fig. 9. In these voltammograms the current peak slightly decrease with the time and it is probably related to the oxidation by the dissolved oxygen of Ferrocenium [14]. However, the couple potential remains practically unchanged justifying the use of Pt wire as RE at least up to 22 h, which is a much longer time compared to the duration of our experiments.

3.2.2. Open circuit voltage curves

The free corrosion potential curves (OCV) were recorded for both the alloys and are shown in Fig. 10. All the systems reach an almost constant potential value after about 9 h of immersion that is −0.32/−0.35 V for the AISI 304 and −0.53/−0.56 V for the AISI1018. These values are the result of superimposed events: the presence of oxidants as dissolved oxygen and the different oxidation states of the metals constituting the alloys. However, the less negative value is shown by the stainless steel (AISI 304), confirming its 'nobler' behaviour in comparison to the carbon steels (AISI 1018).

3.2.3. Potentiodynamic curves

In order to provide information about the active/passive behaviour of the alloys, the potentiodynamic curves were recorded (just after the OCV's) in the range −0.25/1.6 V with respect to the free corrosion potential, at the scan rate
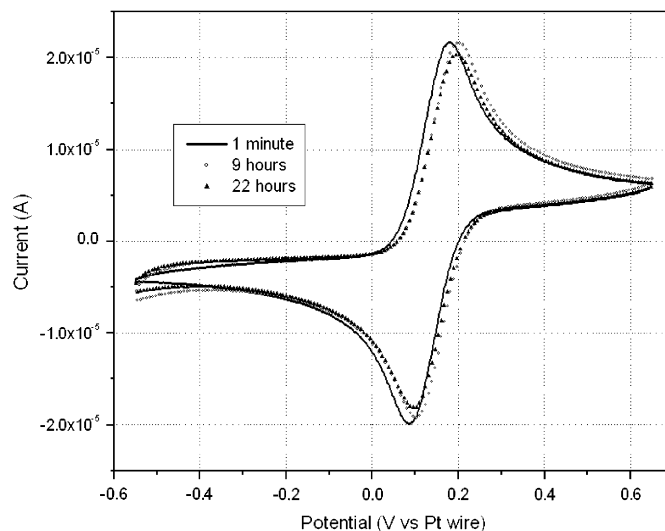

Fig. 9. Cyclic voltammetries (200 mV s^{-1}) of Ferrocene/Ferrocenium couple in EdMPNTf$_2$N, recorded up to the 22th hour following the Ferrocene dissolution.
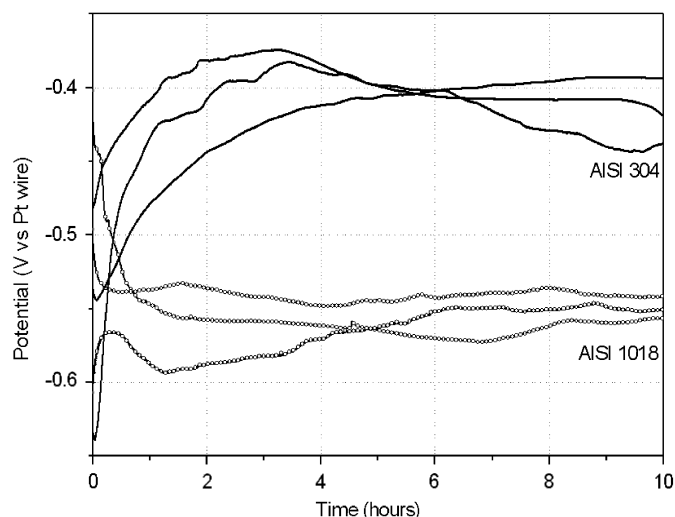
Fig. 10. Room temperature OCV curves of the AISI 304 and the AISI 1018 alloys in EdMPNTf$_2$N. The experiment was performed in open-to-air condition.
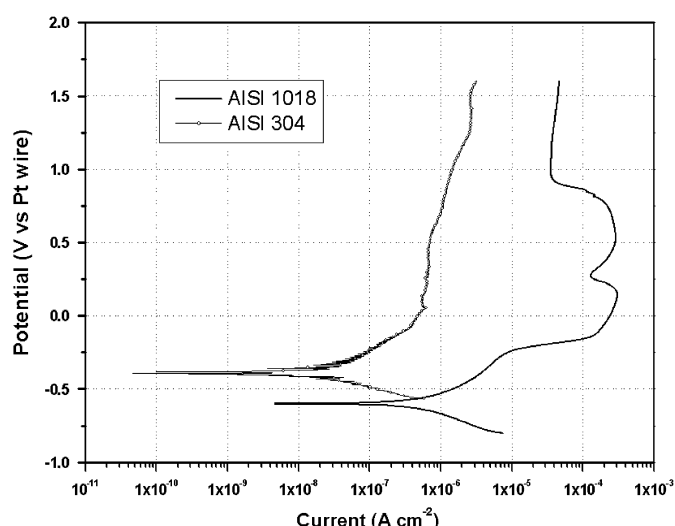

Fig. 11. Room temperature potentiodynamic curves of the AISI 304 and the AISI 1018 in EdMPNTf$_2$N open-to-air condition.

of 1 mV s^{-1} (Fig. 11). AISI 304 shows an active region from about -0.38 up to -0.10 V, while between 0.00 and 0.50 V the current density is almost constant and less than 1 μA cm^{-2}, suggesting a self-passivating behaviour for such alloy.

The AISI 1018 is characterized by a more complex curve; the active region ranges from -0.55 to -0.20 V and the current density displays an increment of about three orders of magnitude with respect to the AISI 304. This high value is consistent with the localized corrosion phenomena that were observed by SEM. The further increment of the potential yields the system to a diffusion limit current density up to 0.75 V, after that, the current decreases again, showing the tendency to form a passive layer.

3.2.4. Tafel plots and polarization resistance measurements

These measurements provide a direct insight into the corrosion current densities of the alloys in ILs environment. After the registration of the OCV curve, polarization resistance (R_{pol}) measurements were performed in the range of ± 25 mV with respect to OCV. After the R_{pol} scan the potential returned to the OCV value in few minutes, at this point, the anodic Tafel plot was recorded starting from -50 up to $+250$ mV with respect to OCV. The cathodic Tafel plot was registered independently, repeating the above-described procedure with fresh ILs and new metal sample. The scan rate for both of these measurements was 0.166 mV s^{-1}.

The slopes of the linear portion of the Tafel plots (β_a and β_c) were used to calculate corrosion current densities. An example of the obtained curves is shown in Fig. 12 while the extrapolated quantities are summarized in Table 2. The values are in good agreement with the data present in literature for similar IL [15,16]. As mentioned before, superimposed events could influence the β values, leading to the observation of a mixed potential.

The results reported here show a complex behaviour of the different combinations of substrate and IL. In several cases, important corrosion phenomena were observed. In general, we believe that the high reactivity of these systems can be at least in part attributed to dissolved oxygen. It appears that ILs can dissolve much more oxygen than water, as recently shown by Brennecke and co-workers [17], which estimates the amount of dissolved oxygen in several ILs, including methyl-tri-butylammonium(Tf$_2$N), which is an IL similar to those employed in this work. According to this study, the Henry's constant expressed in pressure units is about 1000 bar at 25 °C. In comparison, the Henry's constant of oxygen in water, expressed as function of gas concentration and partial pressure is
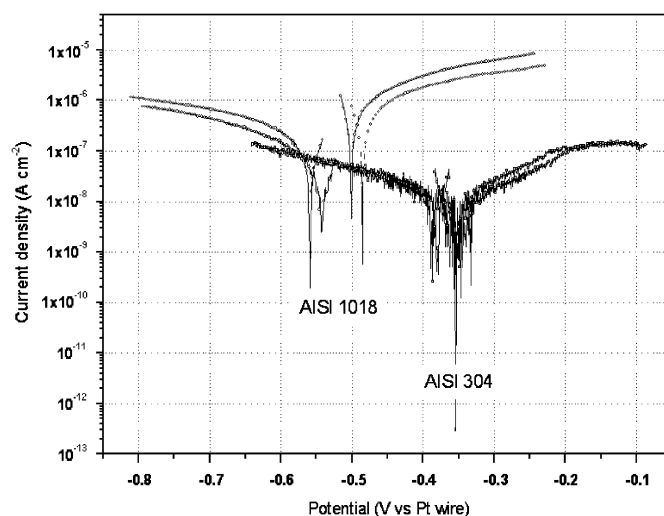

Fig. 12. Room temperature Tafel plots of the AISI 304 and the AISI 1018 steels in EdMPNTf$_2$N. The experiment was performed in open-to-air condition.

Table 2
Electrochemical corrosion data of the investigated alloys at room temperature in EdMPNTf$_2$N

	I_{corr} (An) (μA cm^{-2})	I_{corr} (Cat) (μA cm^{-2})	R_{pol} (Ω)	β_a (mV dec^{-1})	β_c (mV dec^{-1})	I_{corr} R_{pol} (μA cm^{-2})
AISI 304	0.014	0.014	1770×10^3	143	280	0.024
AISI 1018	1.22	0.239	423.8×10^3	127	496	1.17

1.28×10^{-3} mol l^{-1} bar^{-1} at 25 °C:

$$H_{conc} = C_i p i^{-1}. \tag{1}$$

Thus, the oxygen concentration, obtained considering the atmospheric partial pressure of the gas equal to 0.21 bar, is 2.7×10^{-4} M. Since a dm^3 of water contains 55.51 moles, the molar fraction of oxygen is something about 4.86×10^{-6}, that gives rise, according to Eq. (2), to an Henry's constant of 43,210 bar, a pressure 40 times higher to dissolve in water the same amount of oxygen that dissolves in IL.

For the application studied here the laws that govern the electrochemical processes are expressed in terms of molar concentrations. This is not only a formal question. The electrochemistry is not concerned of the relative amount of the solvent and the electroactive species since the solvents only acts as a support for the reaction. The electrochemical phenomena are only affected by the density of the molecules of the electroactive species and of the kinetic of the process. The number of active molecules reaching the electrode surface is related only to the volumetric concentration and also to some combined properties which are functions of both the electrolyte and the electroactive species (e.g. the diffusion coefficient). In terms of molar fraction, the ratio of the solubility of the oxygen in the ionic liquid and in water is large: $43,210/1000 = 43$, but in terms of volume concentration the situation is different, because the number of molecules of solvents per volume unit is different. We have earlier calculated that the oxygen concentration in water is around 0.27 mM or 8.64 mg l^{-1}. For the IL, considering the density of EdMPNTf$_2$N is 1.41 g cm^{-3} and the molar weight is 396.37 g mol^{-1} we can conclude that the number of mol l^{-1} is around 3.5, which is much lower than the 55.5 of water. From the inverse Henry's law, expressed in terms of molar fraction, X_i, and partial pressure, p_i, of the ith gas, we have

$$H_X = p_i X i^{-1} \tag{2}$$

and considering an oxygen partial pressure of 0.21 bar, we get that the molar fraction of dissolved gas is 2.1×10^{-4}. From the definition of molar fraction and considering the number of mol of IL per liter, the concentration of the dissolved oxygen is around 7×10^{-4} mol l^{-1} or 22.4 mg l^{-1}; approximately three times larger than in water. Such a concentration is sufficiently high to justify the occurrence of electrochemical phenomena due to oxygen.

The β values could be also affected by oxidant agents diffusion-controlled mechanism at the electrode interface. Hence, activation polarization contributions seem not negligible. This fact probably is also the cause of the high β values in the cathodic plots (Table 2), where the only reduced agents could be protons from residual water. The determination of the corrosion rates by such electrochemical approach needs the definition of the charge number Z, that, at this moment, can only be a hypothesis. Nevertheless, the comparison of the corrosion current densities derived by the R_{pol} method and the corrosion rates derived by Tafel plots extrapolation shows good agreement. Such element provides a confirmation of the reliability of the performed measurements.

5. Conclusions

The results reported in the present study show that the resistance to corrosion of steel substrates in contact with different ionic liquids (ILs) is still not satisfactory enough for practical applications as heat exchangers in open-to-air condition. Among the investigated ILs only the EdMPNTf$_2$N does not decompose at the working temperature of the trough collectors (220 °C). The other ILs tested decompose and form interaction layers on the surfaces of the steels' samples. Chemical analysis shows these layers are formed principally by the ILs' decomposition products. Regarding EdMPNTf$_2$N, the corrosion current densities are low especially for AISI 304. However, the dissolved oxygen in this IL is not negligible also at the working temperature of the trough collector (220 °C), and therefore, it probably is mainly responsible for the observed corrosion phenomena.

Better resistance to corrosion is likely to be obtainable in absence of air (i.e. nitrogen purged atmosphere), which is a condition that can be obtained in a sealed heat transfer system. The corrosion properties of ILs in controlled atmosphere will be the objective of further investigations in this field.

Acknowledgements

References

[1] SEGS (Solar Electric Generating Station) plants in California's Mojave Desert ⟨http://www.fplenergy.com/⟩ APS, Saguaro power plant, Arizona ⟨http://www.aps.com/general_info/AboutAPS_18.html⟩

Solar power plants in Spain ⟨http://www.solarpaces.org/News/Projects/Spain.htm⟩.

[2] L. Moens, D.M. Blake, D.L. Rudnicki, M.J. Hale, J. Sol. Energy Eng. 125 (2003) 112.

[3] C.P. Fredlake, J.M. Crosthwaite, D.G. Hert, S.N.V.K. Aki, J.F. Brennecke, J. Chem. Eng. Data 49 (2004) 954.

[4] M.E. Van Valkenburg, R.L. Vaughn, M. Williams, J.S. Wilkes, Thermochim. Acta 425 (2005) 181.

[5] M.C. Kroon, W. Buijs, C.J. Peters, G.J. Witkamp, Thermochim. Acta. (2007).

[6] U. Bardi, S.P. Chenakin, S. Caporali, A. Lavacchi, I. Perissi, A. Tolstoguzov, Surf. Interface Anal. 38 (2006) 1768.

[7] M. Kosmulski, J. Gustafsson, J.B. Rosenholm, Thermochim. Acta 412 (2004) 47.

[8] K.J. Baranyai, G.B. Deacon, D.R. MacFarlane, J.M. Pringle, J.L. Scott, Aust. J. Chem. 57 (2004) 145.

[9] Competitive Comparison Report from Duratherm Extended Life Fluids, further information at ⟨http://www.heat-transfer-fluid.com/⟩.

[10] G. Gritzner, J. Kuta, J. Pure Appl. Chem. 56 (1984) 461.

[11] V.M. Hultgren, A.W.A. Mariotti, A.M. Bond, A.G. Wedd, Anal. Chem. 74 (2002) 3151.

[12] S. Eisele, M. Schwarz, B. Speiser, C. Tittel, Electrochim. Acta 51 (2006) 5304.

[13] C. Comminges, R. Barhdadi, M. Lauret, M. Troupel, J. Chem. Eng. Data 51 (2006) 680.

[14] J.K. Bashkin, P.J. Kinlen, Inorg. Chem. 29 (1990) 4507.

[15] M. Arenas, R.G. Reddy, J. Min. Met. 39 (2003) 81.

[16] I. Perissi, U. Bardi, S. Caporali, A. Lavacchi, Corros. Sci. 48 (2006) 2349.

[17] J.L. Anthony, J.L. Anderson, E.J. Maginn, J.F. Brennecke, J. Chem. Phys. B 109 (2005) 6366.